JOC*Note*

Side Reaction of Significance in Preparation of Peptide- or Peptidomimetic-Based Hydroxamate Enzyme Inhibitors

Dusan Hesek, Bruce C. Noll, and Shahriar Mobashery*

Department of Chemistry and Biochemistry, University of Notre Dame, Notre Dame, Indiana 46556

mobashery@nd.edu

Received December 12, 2005

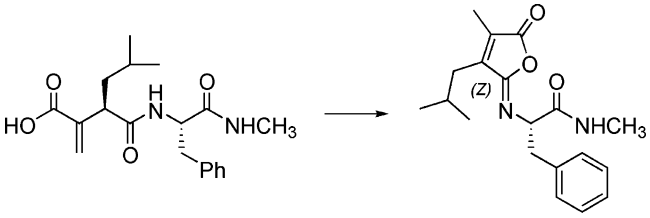

Peptidic and peptidomimetic hydroxamates are increasingly being developed as potential pharmaceutical agents in targeting metalloenzymes. For a number of practical considerations, the hydroxamate moiety is often introduced in the synthesis onto valuable advanced synthetic precursors. The approach entails activation of the carboxylate of the synthetic precursor by any number of methods for the preparation of the hydroxamate. We report herein that this widely used approach in preparation of an entire class of enzyme inhibitors is problematic as documented by the formation of an undesirable cyclization product (characterized in this report), which could at times be the exclusive outcome of the carboxylate activation process.

Hydroxamate inhibitors of enzymes are being made with increased frequency.[1] The hydroxamate moieties of these enzyme inhibitors are usually intended for chelation to active-site metal ions, a function that sequesters the inhibitor within the active site and impairs the catalytic function. Both peptide- and peptidomimetic-based hydroxamates have found considerable use in inhibition of metalloproteinases.[2,3] The concept is that the peptide- or peptidomimetic-based backbone mimics the structural portions of the substrates for these enzymes, whereby the hydroxamate moiety latches the inhibitor onto the active-site metal ion (most often the zinc ion).

Our interest in enzymes that are involved in tumor metastasis has drawn us to the family of matrix metalloproteinases (MMPs). This family of enzymes constitutes a group of 26 closely related proteins that have the ability to alter the extracellular matrix by their functions.[4−9] The functions of these enzymes are strictly regulated under physiological processes. When the cellular regulation is lost, the levels of activities of these enzymes are elevated, an event that causes a number of pathological conditions that include cancer growth, tumor metastasis and angiogenesis, arthritis, connective tissue diseases, inflammation, and cardiovascular, neurological, and autoimmune diseases.[10−16] As such, many inhibitor design programs have targeted MMPs.[3,7,17−20]

Our efforts in the area of MMP inhibition necessitated synthesis of batimastat (**5**) in large quantities. This is a broad-spectrum and highly potent inhibitor of MMPs. The synthesis of this compound has appeared only in the patent literature (Scheme 1).[21,22] The synthesis is a multistep process starting from D-leucine (**1**), progressing through the intermediary compounds **2**−**4**. As the final step, the precursor **4** is coupled to hydroxylamine to afford batimastat (**5**).

The direct conversion of carboxylic acid **4** to the corresponding hydroxamic acid derivative **5** was performed with an excess of either hydroxylamine or *O*-silyl hydroxylamine using an EDCI-mediated coupling protocol in the presence of HOBt at 4 °C. Although the reactions proceeded in moderate yields, the presence of base readily initiates an elimination of the labile thienylthio functionality, which in turn resulted in undesired side products together with the formation of the corresponding acrylate intermediate **3**. To improve the outcome of this reaction, we tried alternative coupling methods (e.g., DCC, $POCl_3$, and pivaloyl-mixed anhydride) starting from **4**, all of which at the end proved unsatisfactory.

The difficulties in the final step were serious, as the precious key precursor **4** was not giving the desired product in sufficient purity and acceptable yields. The patent literature precedents in this area lack sufficient details on the procedures,[21,22] prompting us to investigate the root cause of the difficulty. We wondered if the activation step for the amide bond formation in the presence of a thienylthiomethyl substituent was the problem. We envisioned that activation of the carboxylic

(1) Leung, D.; Abbenante, G.; Fairlie, D. P. *J. Med. Chem.* **2000**, *43*, 305−341.
(2) Matthews, B. W. *Acc. Chem. Res.* **1988**, *21*, 333−340.
(3) Whittaker, M.; Floyd, C. D.; Brown, P.; Gearing, A. J. H. *Chem. Rev.* **1999**, *99*, 2735−2776.
(4) Coussens, L. M.; Fingleton, B.; Matrisian, L. M. *Science* **2002**, *295*, 2387−2392.
(5) Doherty, T. M.; Asotra, K.; Pei, D. Q.; Uzui, H.; Wilkin, D. J.; Shah, P. K.; Rajavashisth, T. B. *Expert Opin. Ther. Pat.* **2002**, *12*, 665−707.
(6) Egeblad, M.; Werb, Z. *Nat. Rev. Cancer* **2002**, *2*, 161−174.
(7) Lee, M.; Fridman, R.; Mobashery, S. *Chem. Soc. Rev.* **2004**, *33*, 401−409.
(8) Massova, I.; Kotra, L. P.; Fridman, R.; Mobashery, S. *FASEB J.* **1998**, *12*, 1075−1095.
(9) Overall, C. M.; Lopez-Otin, C. *Nat. Rev. Cancer* **2002**, *2*, 657−672.
(10) Bergers, G.; Benjamin, L. E. *Nat. Rev. Cancer* **2003**, *3*, 401−410.
(11) Forget, M.-A.; Desrosiers, R. R.; Beliveau, R. *Can. J. Physiol. Pharmacol.* **1999**, *77*, 465−480.
(12) Hanahan, D.; Weinberg, R. A. *Cell* **2000**, *100*, 57−70.
(13) Kerbel, R.; Folkman, J. *Nat. Rev. Cancer* **2002**, *2*, 727−739.
(14) Nelson, A. R.; Fingleton, B.; Rothenberg, M. L.; Matrisian, L. M. *J. Clin. Oncol.* **2000**, *18*, 1135−1149.
(15) Steeg, P. S. *Nat. Med.* **2003**, *9*, 822−823.
(16) Van't Veer Laura, J.; Weigelt, B. *Nat. Med.* **2003**, *9*, 999−1000.
(17) Buolamwini, J. K. *Curr. Opin. Chem. Biol.* **1999**, *3*, 500−509.
(18) Cristofanilli, M.; Charnsangavej, C.; Hortobagyi, G. N. *Nat. Rev. Drug Discov.* **2002**, *1*, 415−426.
(19) Rao, B. G. *Curr. Pharm. Des.* **2005**, *11*, 295−322.
(20) Skiles, J. W.; Gonnella, N. C.; Jeng, A. Y. *Curr. Med. Chem.* **2001**, *8*, 425−474.
(21) Campion, C.; Davidson, A. H.; Dickens, J. P.; Crimmin, M. J. *PCT Int. Appl.*; British Bio-Technology Ltd.: U.K., 1990, WO9005719.
(22) Sakamoto, M.; Imaoka, T.; Motoyama, M.; Yamamoto, Y.; Takasu, H. *PCT Int. Appl.*; Otsuka Pharmaceutical Co., Ltd.: Japan, 1994, WO9421612.

10.1021/jo052546f CCC: $33.50
Published on Web 02/28/2006

SCHEME 1

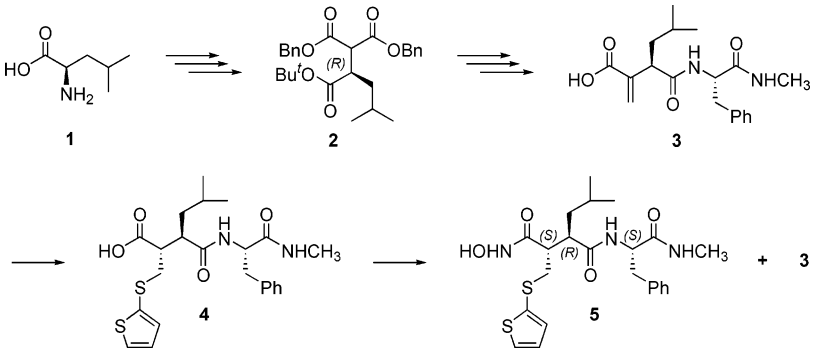

SCHEME 2

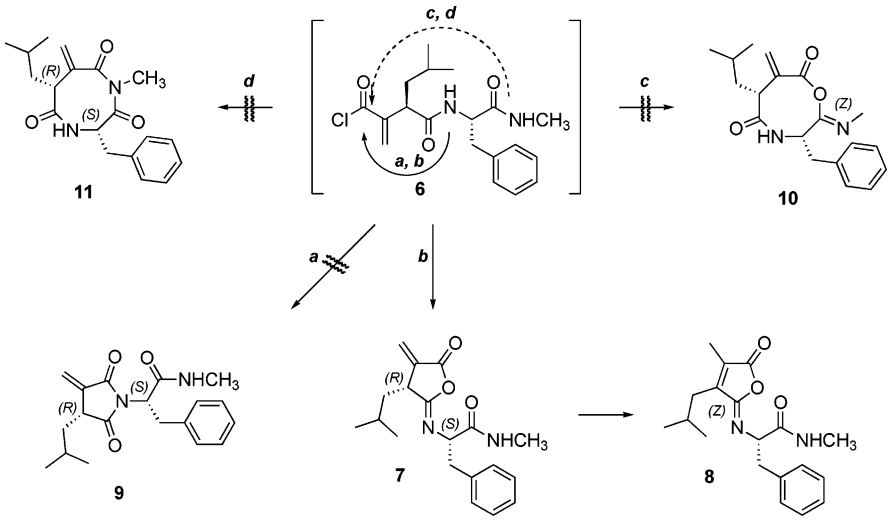

function of the α,*β*-unsaturated derivative **3** could either eliminate side-product formations or serve as an appropriate intermediate for regioselective introduction of a hydroxylamido functionality at the terminal carboxyl group. Therefore, the direct conversion of carboxylic acid **3** to the corresponding hydroxamic acid derivative was performed.

The reaction of the carboxylic acid **3** with EDCI/HOBt was done at 4 °C to give an intermediate, the identity of which could not be established by NMR and mass spectrometric analyses. However, when this reactive intermediate was treated in situ with hydroxylamine, to our surprise, it did not give the expected corresponding hydroxamate derivative, but instead a novel product. Interestingly, the very same product was obtained in quantitative yield during the preparation of **6**, for which we used oxalyl chloride and **3** in the presence of triethylamine. The likely outcomes for the reaction are depicted in Scheme 2. The expected species would presumably arise by the intramolecular attack of the acyl chloride in **6** (or any myriad of activated carboxylic acids) by the internal amide groups, to form five- (pathway a and b, Scheme 2) or eight-membered ring systems (pathway c and d), respectively. As noted earlier, only one product was seen (regardless of the nature of the carboxylate activation), which was characterized by NMR (including COSY, HMQC, and HMBC experiments) and by MS, which produced data consistent with **8** as the structure. Crystals of the compound were grown by diffusion of ether into a chloroform solution of the crude synthetic material, and X-ray diffraction analysis was performed to elucidate the structure unambiguously (see Figure 1). The stereochemistry for the chiral center was assigned on the basis of the X-ray diffraction analysis and was correlated with stereochemistry of the starting material. Spectroscopic studies, capped by an X-ray crystallographic analysis, established the compound unambiguously as **8**. Crystal data, atomic coordinates, bond lengths, and angles for **8** are given in Tables 1−6 of the Supporting Information.

Although we could not isolate the reaction intermediates **6** and **7**, it would be reasonable to assume that **8** was produced exclusively by the facile rearrangement of derivative **7**. We propose that the reaction sequence is initiated by intramolecular cyclization via pathway b (Scheme 2) affording **7**, which is then converted by prototropic rearrangement into the thermodynamically more stable isoimide **8**. The preferential attack of the less nucleophilic oxygen of the amide functionality occurs at the activated carboxylate, which interestingly proceeds with complete regioselectivity to furnish exclusively (*Z*)-isoimide derivative **8**. The formation of the imide derivative **9** would have been intuitively reasonable, but it is not seen. In view of this observation, the transition state of the critical cyclization step would appear to be influenced by steric factors rather than by the competitive nucleophilicities of the oxygen vs the nitrogen of the amide of **6**. All attempts at isolation of alternative derivatives having eight-membered 1,4-oxazocane (**10**, pathway c) or 1,4-diazocane (**11**) heterocyclic ring systems (pathway d) by varying the reaction conditions or by quenching reaction mixtures with different solvents such as *n*-hexane or ethanol were unsuccessful.

With **8** in hand, we reanalyzed samples from previous disparate synthetic approaches to **5** that we had employed. All

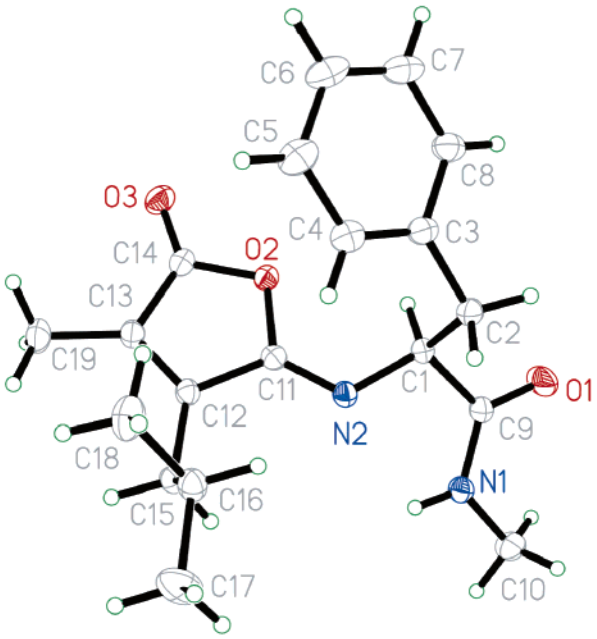

FIGURE 1. ORTEP drawing of isoimide **8**, drawn at 50% probability level.

these reaction mixtures indicated the presence of **8** to varying degrees. Therefore, this significant side reaction is a major contaminant in the synthesis of batimastat. Considering that its formation takes place at the end of a multistep synthesis with a valuable synthetic precursor, the known synthetic routes to batimastat and related compounds are problematic.

In retrospect, the outcome of this side reaction should not be totally unanticipated. However, in light of the desirability of both peptidic and peptidomimetic hydroxamate derivatives as enzyme inhibitors and as potential pharmaceuticals, effective routes to their preparations should be devised. Because activation of carboxylates for the formation of hydroxamates late into the synthetic scheme would appear to be preferred, the synthetic scheme should be devised such that the undesired cyclization process could be avoided. The significance of this side reaction cannot be discounted as it could proceed as the exclusive outcome of the reaction of the activated carboxylate in some cases.

Experimental Section

Synthesis of (2*S*)-2-[(2*Z*)-3-Isobutyl-4-methyl-5-oxofuran-2(5*H*)-ylideneamino]-*N*-methyl-3-phenylpropan-amide (8). A 25 mL flask was charged with **3** (0.7 g, 2 mmol) under nitrogen, followed by the addition of dichloromethane (10 mL). The solution was cooled to −5 to 0 °C, and oxalyl chloride (2.0 M) in CH_2Cl_2 (0.4 mL) was added over 5 min, followed by anhydrous DMF (0.15 mL), while the internal temperature was maintained just below −5 °C. The reaction mixture was stirred at 0 °C for an additional 15 min to give a solution of the acyl chloride **6**.

A stirred suspension of hydroxylamine hydrochloride (0.48 g, 7 mmol) in CH_2Cl_2 (10 mL) and 1,8-diazabicyclo[5.4.0]undec-7-ene (DBU, 1.1 g, 7 mmol) was mixed with the solution of acyl chloride **6** via cannula while maintaining the internal temperature between −5 and 0 °C. The mixture was stirred for 2 h under an atmosphere of nitrogen, and then it was quenched by the addition of water (4 mL) and extracted with dichloromethane. The organic phase was concentrated to a residue, which was flash chromatographed (eluent; $CHCl_3$/MeOH = 8:2) to give the title compound **8** as a white solid (0.61 g, 87% yield). ^{1}H NMR (500 MHz, $CDCl_3$): δ ppm 0.90 (d, J = 6.55 Hz, 3H), 0.98 (d, J = 6.89 Hz, 3H), 1.94 (s, 3H), 1.95−2.00 (m, 1H), 2.27−2.42 (m, 2H), 2.86 (d, J = 5.17 Hz, 3H), 3.01 (dd, J = 13.44, 8.61 Hz, 1H), 3.39 (dd, J = 13.44, 3.79 Hz, 1H), 4.70 (dd, J = 8.44, 3.96 Hz, 1H), 6.62 (d, J = 3.79 Hz, 1H), 7.11 (d, J = 6.89 Hz, 2H), 7.16−7.23 (m, 3H).^{13}C NMR (126 MHz, $CDCl_3$): δ ppm 9.2, 22.1, 22.8, 25.9, 28.1, 33.4, 40.4, 63.4, 126.5, 127.8, 129.4, 133.6, 136.8, 147.9, 153.5, 167.2, 171.4. LC/MS *m*/*z* 329 (M + 1).

Crystal Growth and Analysis. Compound **8** (300 mg) in chloroform (5 mL) was heated to produce a clear, colorless solution. Crystals of suitable size for single-crystal X-ray diffraction analysis were obtained by diffusion of diethyl ether into the chloroform solution at room temperature overnight. Cell parameters were determined using reflections harvested from three sets of 120.5° φ scans. The orientation matrix derived from this was passed to COSMO[23] to determine the optimum data collection strategy. Average 7.4-fold redundancy was achieved using 11 ω scan series and 6 φ scan series. Data were measured to 0.68 Å. Cell parameters were refined using 9126 reflections with $I \geq 10\sigma(I)$ and 2.611° ≤ θ ≤ 31.507° harvested from the entire data collection. In total, 46 162 reflections were measured, 3208 unique and 3178 observed, $I > 2\sigma(I)$. All data were corrected for Lorentz and polarization effects, and runs were scaled using SADABS[24] with the "no absorption" option.

The structure was solved using direct methods in monoclinic space group $P2_1$. All non-hydrogen atoms were assigned after the initial solution. Hydrogens were placed at calculated geometries and allowed to ride on the position of the parent atom. Hydrogen thermal parameters were set to 1.2 times the equivalent isotropic U of the parent atom and to 1.5 times that for methyl hydrogens. The hydrogen bound to N1 was located by difference map and freely refined in subsequent cycles of least-squares refinement. Non-hydrogen atoms were refined with parameters for anisotropic thermal motion. The largest peak in the final difference map, 0.35 $e^-\cdot Å^{-3}$, was located on the midpoint of the C12−C13 bond. All of the 10 largest peaks were situated along bonds. The electron density varied from 0.35 to 0.27 $e^-\cdot Å^{-3}$. Stereochemistry was assigned from a stereocenter that was unchanged through the reaction. The Flack parameter,[25] though not definitive for light-atom structures and Mo Kα radiation, was in agreement with the assigned stereochemistry. The Flack parameter refined to 0.13(10) for the reported structure and to 0.87(10) for the inverted structure.

Supporting Information Available: Tables of atomic positions, thermal parameters, and bond lengths and angles, as well as full crystallographic data for **8** (CIF); NMR spectra for the synthetic molecules **3** and **8**. This material is available free of charge via the Internet at http://pubs.acs.org.

JO052546F

(23) *COSMO*; Bruker-AXS: Madison, WI, 2004.
(24) Sheldrick, G. M. *SADABS*; University of Göttingen: Germany, 2004.
(25) Flack, H. D. *Acta Crystallogr., Sect. A: Found. Crystallogr.* **1983**, *39*, 876−881.